07.2;09.1

Features of the iron charge states in semi-insulating β-Ga_2O_3:Fe identified by high-frequency electron paramagnetic resonance

© R.A. Babunts, A.S. Gurin, E.V. Edinach, Yu.A. Uspenskaya, P.G. Baranov

Ioffe Institute, St. Petersburg, Russia
E-mail: yulia.uspenskaya@mail.ioffe.ru

Received July 12, 2023
Revised September 13, 2023
Accepted September 13, 2023

The charge states of non-Kramers Fe^{2+} ions and Fe^{3+} ions in the octahedral and tetrahedral positions of the crystal lattice in a commercial substrate of semi-insulating gallium oxide β-Ga_2O_3 before and after proton irradiation with an energy of 15 MeV have been identified by high-frequency EPR.

Keywords: electron paramagnetic resonance (EPR), semiconductors, gallium oxide.

DOI: 10.61011/TPL.2023.11.57189.19685

β-gallium oxide (β-Ga_2O_3) is a wideband semiconductor with a band gap on the order of 4.8 eV. Both single crystals and thin films of β-Ga_2O_3 are currently being fabricated for applications ranging from power electronics to solar-blind detectors [1–5]. One of the advantages of the Ga_2O_3 system is high radiation resistance, which makes it suitable for application in the space environment [6,7]. Experiments into the influence of radiation effects on the properties of crystals, films, and devices based on Ga_2O_3 have been performed for β-Ga_2O_3 [6,8]. The variation of electric, luminescent, and recombination properties under irradiation with protons, neutrons, α particles, and γ particles has been examined in detail. In certain cases, the nature of defects was identified based on the results of comparison with comprehensive theoretical modeling data [6,8,9].

Iron is an important dopant impurity for the fabrication of semi-insulating β-Ga_2O_3 substrates and is present in trace amounts ($10^{16}-10^{17}\,cm^{-3}$) almost in all grown bulk β-Ga_2O_3 crystals (due to its presence in the initial materials). Numerous studies of the optical and electric properties of iron ions in this essential semiconductor [10–14] have been performed by several research groups for the purpose of enhancing the performance of new devices.

Electron paramagnetic resonance (EPR) is one of the most informative methods for identification of ions of transition metals (including iron) in different charge states in semiconductors. The Fermi level position has a major effect on the manifestation of different charge states. We have recently published the results of EPR studies of nominally undoped bulk β-Ga_2O_3 crystals [15], where the Fermi level position, which was altered via irradiation with electrons, was demonstrated to be one of the key parameters specifying the charge and spin states of transition elements. In addition to EPR spectra of the known Fe^{3+} charge state, EPR spectra of state Fe^{2+} were detected. Indirect indications of the possibility of existence of this state have earlier been the subject of wide discussion [16,17]. The giant splitting of spin levels in zero magnetic field, which is attributable to the fact that Fe^{2+} ions (so-called non-Kramers ions) have an integer total spin $S = 2$, is a specific feature of EPR spectra of these ions. This precluded the researchers from detecting them with EPR spectrometers operating in common bands. Measurements were performed with the use of a high-frequency EPR spectrometer designed at the Ioffe Institute in collaboration with LTD „DOK“ (St. Petersburg, Russia). This spectrometer, which operates both in continuous-wave and pulse modes, is based on a line of microwave bridges (94 and 130 GHz) and a fully autonomous closed-cycle magneto-optical cryogenic system that allows one to vary the temperature within the 1.5−300 K range [18,19]. A commercial JEOL JES-PE-3 EPR spectrometer operating in the continuous-wave mode in the X band was also used.

The examined semi-insulating crystals of gallium oxide doped with iron were commercial samples produced by Kyma Technologies (United States). They were grown by the Czochralski method with Fe_2O_3 introduced into the initial material with a Fe^{3+} concentration on the order of $(2-3)\cdot 10^{19}\,cm^{-3}$. These samples were irradiated with protons with an energy of 15 MeV and a dose of $\sim 10^{16}\,cm^{-2}$ at room temperature. Since semi-insulating β-Ga_2O_3 is highly resistant to radiation, the shape of EPR spectra and the line intensities remained unchanged after irradiation.

Figure 1 presents the orientation dependence of EPR signals of a Fe^{3+} ion in a semi-insulating Ga_2O_3:Fe crystal detected in the continuous-wave mode at a frequency of 9.5 GHz at room temperature. Only the EPR spectra of Fe^{3+} ions, which are characterized by spin $S = 5/2$ (electron configuration $3d^5$), are seen at this frequency. These Fe^{3+} ions substitute gallium and occupy both octahedral and tetrahedral sites in the gallium lattice.

The EPR spectra measured at high frequencies of 94 and 130 GHz provide a more complete picture. Figure 2 presents the orientation dependence of EPR signals of Fe^{3+} and Fe^{2+} ions in a semi-insulating Ga_2O_3:Fe crystal detected

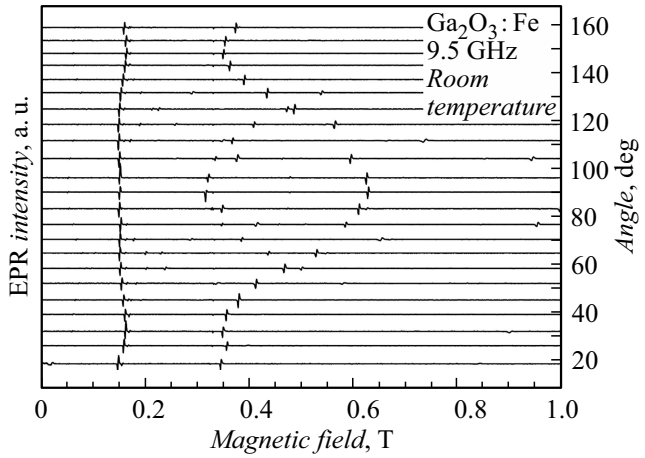

Figure 1. Orientation dependence of EPR signals of a Fe^{3+} ion in a semi-insulating Ga_2O_3:Fe crystal detected in the continuous-wave mode at a frequency of 9.5 GHz at room temperature.

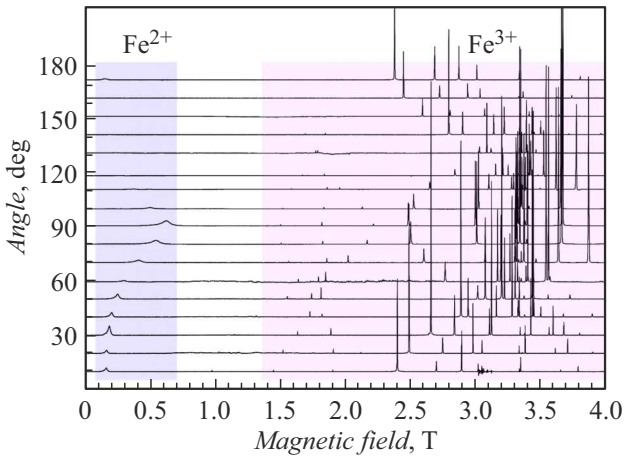

Figure 2. Orientation dependence of EPR signals of Fe^{3+} and Fe^{2+} ions in a semi-insulating Ga_2O_3:Fe crystal detected in the continuous-wave mode at a frequency of 94 GHz at a temperature of 4 K.

in the continuous-wave mode at a frequency of 94 GHz at a temperature of 4 K.

A significant asymmetry of intensities of EPR lines with respect to the center in the $g = 2$ region is observed in the EPR spectra of Fe^{3+} ions. This is attributable to the Boltzmann distribution of populations of spin levels. One may gain a better understanding of these EPR spectra by examining Fig. 3, which shows the fragment of EPR spectra of Fe^{3+} ions detected in the continuous-wave mode at low (4 K) and high (100 K) temperatures. It is evident that the high-temperature spectrum is almost symmetric with respect to its center, since the influence of the Boltzmann factor is greatly decreased. The fine structure of lines for Fe^{3+} ions in octahedral and tetrahedral positions is also seen.

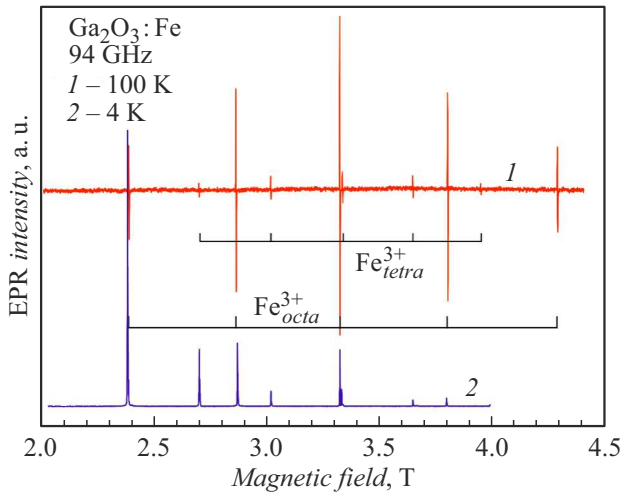

Figure 3. EPR spectra of a Fe^{3+} ion in a semi-insulating Ga_2O_3:Fe crystal detected in the continuous-wave mode at a frequency of 94 GHz at temperatures of 100 (*1*) and 4 K (*2*). The fine structure of lines for Fe^{3+} ions in octahedral and tetrahedral positions is indicated.

The observed EPR spectra were characterized using a reduced spin Hamiltonian in standard form

$$H = \mu_B \mathbf{B} \cdot \mathbf{g} \cdot \mathbf{S} + D\left[\mathbf{S}_z^2 - \frac{1}{3}S(S+1)\right] + E\left[\mathbf{S}_x^2 - \mathbf{S}_y^2\right],$$

where $S = 5/2$ for Fe^{3+} (electron configuration $3d^5$). The first term characterizes the Zeeman interaction with an anisotropic g-factor represented by a **g**-tensor (μ_B is the Bohr magneton). The second and the third terms correspond to the fine structure interaction, which induces the splitting of energy levels in zero magnetic field. Parameter D incorporates the contribution of the z-axis part of the crystalline field, while parameter E does the same for the axis part.

The observed EPR spectra were modeled in EasySpin [20]. EPR spectra of Fe^{3+} ions in octahedral positions with $D = 6.6$ GHz, $E = -2.55$ GHz, and $\mathbf{g} = [2.004, 2.002, 2.007]$ and spectra of Fe^{3+} ions in tetrahedral positions with $D = 4.4$ GHz, $E = -1.8$ GHz, and $\mathbf{g} = [2.004, 2.002, 2.007]$ were simulated.

Thus, it was established unambiguously that two charge states of iron (Fe^{2+} and Fe^{3+}) are present in a semi-insulating material and that the spectra detected earlier belong to iron ions. Further studies into variations of the Fermi level position under the influence of different doses of irradiation should clarify the energy parameters of positioning of iron levels in the band gap and the relative positioning of iron levels at different crystallographic sites. It should also be noted that the shape of EPR spectra and the line intensities remained unchanged after irradiation with protons with an energy of 15 MeV and a dose of $\sim 10^{16}$ cm^{-2}, indicating that semi-insulating β-gallium oxide is highly resistant to radiation.

Acknowledgments

The authors wish to thank V.I. Safarov for fruitful cooperation, valuable and constructive suggestions, and in-depth discussion of results.

Funding

This study was supported by grant No. 22-12-00003 from the Russian Science Foundation, https://rscf.ru/project/22-12-00003/

Conflict of interest

The authors declare that they have no conflict of interest.

References

[1] S.J. Pearton, J. Yang, P.H. Cary, F. Ren, J. Kim, M.J. Tadjer, M.A. Mastro, Appl. Phys. Rev., **5**, 011301 (2018). DOI: 10.1063/1.5006941
[2] S.J. Pearton, F. Ren, M. Tadjer, J. Kim, J. Appl. Phys., **124**, 220901 (2018). DOI: 10.1063/1.5062841
[3] M. Baldini, Z. Galazka, G. Wagner, Mater. Sci. Semicond. Process., **78**, 132 (2018). DOI: 10.1016/j.mssp.2017.10.040
[4] Z. Liu, P.-G. Li, Y.-S. Zhi, X.-L. Wang, X.-L. Chu, W.-H. Tang, Chin. Phys. B, **28**, 017105 (2019). DOI: 10.1088/1674-1056/28/1/017105
[5] X.H. Chen, F.F. Ren, S.L. Gu, J.D. Ye, Photon. Res., **7**, 381 (2019). DOI: 10.1364/PRJ.7.000381
[6] J. Kim, S.J. Pearton, C. Fares, J. Yang, F. Ren, S. Kim, A.Y. Polyakov, J. Mater. Chem. C, **7**, 10 (2019). DOI: 10.1039/C8TC04193H
[7] S.J. Pearton, A. Aitkaliyeva, M. Xian, F. Ren, A. Khachatrian, A. Ildefonso, Z. Islam, M.A.J. Rasel, A. Haque, A.Y. Polyakov, J. Kim, ECS J. Solid State Sci. Technol., **10**, 055008 (2021). DOI: 10.1149/2162-8777/abfc23
[8] E. Ahmadi, Y. Oshima, J. Appl. Phys., **126**, 160901 (2019). DOI: 10.1063/1.5123213
[9] M.E. Ingebrigtsen, A.Yu. Kuznetsov, B.G. Svensson, G. Alfieri, A. Mihaila, U. Badstübner, A. Perron, L. Vines, J.B. Varley, APL Mater., **7**, 022510 (2019). DOI: 10.1063/1.5054826
[10] A.Y. Polyakov, N.B. Smirnov, I.V. Shchemerov, S.J. Pearton, F. Ren, A.V. Chernykh, A.I. Kochkova, Appl. Phys. Lett., **113**, 142102 (2018). DOI: 10.1063/1.5051986
[11] A.T. Neal, S. Mou, S. Rafique, H. Zhao, E. Ahmadi, J.S. Speck, K.T. Stevens, J.D. Blevins, D.B. Thomson, N. Moser, K.D. Chabak, G.H. Jessen, Appl. Phys. Lett., **113**, 062101 (2018). DOI: 10.1063/1.5034474
[12] A.Y. Polyakov, N.B. Smirnov, I.V. Schemerov, A.V. Chernykh, E.B. Yakimov, A.I. Kochkova, A.N. Tereshchenko, S.J. Pearton, ECS J. Solid State Sci. Technol., **8**, Q3091 (2019). DOI: 10.1149/2.0171907jss
[13] S. Bhandari, M.E. Zvanut, J.B. Varley, J. Appl. Phys., **126**, 165703 (2019). DOI: 10.1063/1.5124825
[14] A.Y. Polyakov, N.B. Smirnov, I.V. Shchemerov, A.A. Vasilev, E.B. Yakimov, A.V. Chernykh, A.I. Kochkova, P.B. Lagov, Yu.S. Pavlov, O.F. Kukharchuk, A.A. Suvorov, N.S. Garanin, I.-H. Lee, M. Xian, F. Ren, S.J. Pearton, J. Phys. D: Appl. Phys., **53**, 274001 (2020). DOI: 10.1088/1361-6463/ab83c4
[15] R.A. Babunts, A.S. Gurin, E.V. Edinach, H.-J. Drouhin, V.I. Safarov, P.G. Baranov, J. Appl. Phys., **132**, 155703 (2022). DOI: 10.1063/5.0102147
[16] C.A. Lenyk, T.D. Gustafson, L.E. Halliburton, N.C. Giles, J. Appl. Phys., **126**, 245701 (2019). DOI: 10.1063/1.5133051
[17] T.D. Gustafson, C.A. Lenyk, L.E. Halliburton, N.C. Giles, J. Appl. Phys., **128**, 145704 (2020). DOI: 10.1063/5.0021756
[18] E.V. Edinach, Yu.A. Uspenskaya, A.S. Gurin, R.A. Babunts, H.R. Asatryan, N.G. Romanov, A.G. Badalyan, P.G. Baranov, Phys. Rev. B, **100**, 104435 (2019). DOI: 10.1103/PhysRevB.100.104435
[19] R.A. Babunts, A.G. Badalyan, A.S. Gurin, N.G. Romanov, P.G. Baranov, A.V. Nalivkin, L.Yu. Bogdanov, D.O. Korneev, Appl. Magn. Reson., **51**, 1125 (2020). DOI: 10.1007/s00723-020-01235-9
[20] S. Stoll, A. Schweiger, J. Magn. Reson., **178**, 42 (2006). DOI: 10.1016/j.jmr.2005.08.013

Translated by D.Safin